Formation of heavy d-electron quasiparticles in Sr3Ru2O7

Allan, M.P.; Tamai, A.; Rozbicki, E.; Fischer, M.H.; Voss, .J.; King, P.D.C.; ... ; Baumberger, F.

New Journal of Physics
The open access journal at the forefront of physics

Deutsche Physikalische Gesellschaft DPG IOP Institute of Physics

PAPER • OPEN ACCESS

Formation of heavy d-electron quasiparticles in $Sr_3Ru_2O_7$

To cite this article: M P Allan *et al* 2013 *New J. Phys.* **15** 063029

New Journal of Physics
The open access journal for physics

Formation of heavy d-electron quasiparticles in $Sr_3Ru_2O_7$

M P Allan[1,2,11], A Tamai[1,12], E Rozbicki[1], M H Fischer[2], J Voss[3], P D C King[1], W Meevasana[1,4], S Thirupathaiah[5], E Rienks[5], J Fink[5,6], D A Tennant[7], R S Perry[1], J F Mercure[1], M A Wang[2], Jinho Lee[2,8], C J Fennie[3], E-A Kim[2], M J Lawler[2,9], K M Shen[2], A P Mackenzie[1], Z-X Shen[10] and F Baumberger[1,12]

[1] SUPA, School of Physics and Astronomy, University of St Andrews, St Andrews, Fife KY16 9SS, UK
[2] LASSP, Department of Physics, Cornell University, Ithaca, NY 14853, USA
[3] School of Applied and Engineering Physics, Cornell University, Ithaca, NY 14853, USA
[4] School of Physics, Suranaree University of Technology, Nakhon Ratchasima 30000, Thailand
[5] Helmholtz-Zentrum Berlin, Elektronenspeicherring BESSY II, D-12489 Berlin, Germany
[6] IFW Dresden, PO Box 270116, D-01171 Dresden, Germany
[7] Helmholtz-Zentrum Berlin, Hahn-Meitner-Platz 1, D-14109 Berlin, Germany
[8] Department of Physics and Astronomy, Seoul National University, Seoul 151-747, Korea
[9] Department of Physics, Binghamton University, Binghamton, NY 13902, USA
[10] Departments of Applied Physics, Physics, and Stanford Synchrotron Radiation Laboratory, Stanford University, Stanford, CA 94305, USA
E-mail: milan.allan@gmail.com

New Journal of Physics **15** (2013) 063029 (10pp)
Received 20 February 2013
Published 20 June 2013
Online at http://www.njp.org/
doi:10.1088/1367-2630/15/6/063029

[11] Author to whom any correspondence should be addressed.
[12] Present address: Département de Physique de la Matière Condensée, Université de Genève, 24 Quai Ernest-Ansermet, 1211 Genève 4, Switzerland.

Abstract. The phase diagram of $Sr_3Ru_2O_7$ shows hallmarks of strong electron correlations despite the modest Coulomb interaction in the Ru 4d shell. We use angle-resolved photoelectron spectroscopy measurements to provide microscopic insight into the formation of the strongly renormalized heavy d-electron liquid that controls the physics of $Sr_3Ru_2O_7$. Our data reveal itinerant Ru 4d-states confined over large parts of the Brillouin zone to an energy range of <6 meV, nearly three orders of magnitude lower than the bare band width. We show that this energy scale agrees quantitatively with a characteristic thermodynamic energy scale associated with quantum criticality and illustrate how it arises from a combination of back-folding due to a structural distortion and the hybridization of light and strongly renormalized, heavy quasiparticle bands. The resulting heavy Fermi liquid has a marked **k**-dependence of the renormalization which we relate to orbital mixing along individual Fermi surface sheets.

The unusual physics of the bilayer ruthenate $Sr_3Ru_2O_7$ exemplifies some of the unsolved problems in condensed matter physics. Its rich phase diagram includes quantum criticality, magnetism and an electron nematic phase [1–5] and has generated considerable theoretical interest [6–17]. While there is no consensus on the precise microscopic origin of these properties, they are often associated with an instability of a heavy Fermi liquid resulting from strong correlations and the existence of a low-energy scale of unknown origin. This is consistent with the high electronic specific heat coefficient of $\gamma \sim 110\,\mathrm{mJ/mol\,RuK^2}$ of $Sr_3Ru_2O_7$ [18] and with recent angle-resolved photoemission spectroscopy (ARPES) [19], scanning tunneling microscopy (STM) [20, 21] and quantum oscillation measurements [22] that all indicate the existence of itinerant electrons with high quasiparticle masses. However, little is known about the structure of the heavy Fermi liquid and the origin of the putative low-energy scale in $Sr_3Ru_2O_7$. Within density functional theory in the local density approximation (LDA), $Sr_3Ru_2O_7$ has a wide bare conduction band, formed by relatively extended Ru 4d states hybridizing with O 2p electrons and a similar density of states at the Fermi level as the single-layer compound Sr_2RuO_4. Yet, the latter has remarkably different physical properties and a much smaller electronic specific heat indicative of weaker correlations than in $Sr_3Ru_2O_7$. Recent dynamical mean field theory studies of generic trends in transition metal oxides [23–25] show strong correlation effects at low frequencies in ruthenates but the difference between $Sr_3Ru_2O_7$ and Sr_2RuO_4 remains largely unexplored.

The existence of the low-energy scale in $Sr_3Ru_2O_7$ mentioned above is supported by recent transport and entropy data [2, 5]. Relevant in the context of this paper is the observation of a maximum in the zero-field electronic specific heat $C_{el}(T)/T$ near 8 K. The position of this maximum can be suppressed continuously in an external field, terminating in a logarithmic divergence at the putative quantum critical end point [5]. This suggests that criticality in $Sr_3Ru_2O_7$ is driven by the suppression of a single, low-energy scale that persists in zero field. However, despite recent progress in characterizing the low-energy electronic structure of $Sr_3Ru_2O_7$ [19–21], the microscopic origin of this energy scale remained elusive.

Here, we report detailed ARPES measurements of $Sr_3Ru_2O_7$ revealing flat Ru 4d bands that define an energy scale consistent with thermodynamic measurements. We show how this energy scale arises microscopically from the hybridization of strongly renormalized bands with dispersive states. The resulting Fermi liquid shows pronounced multi-band effects and has a

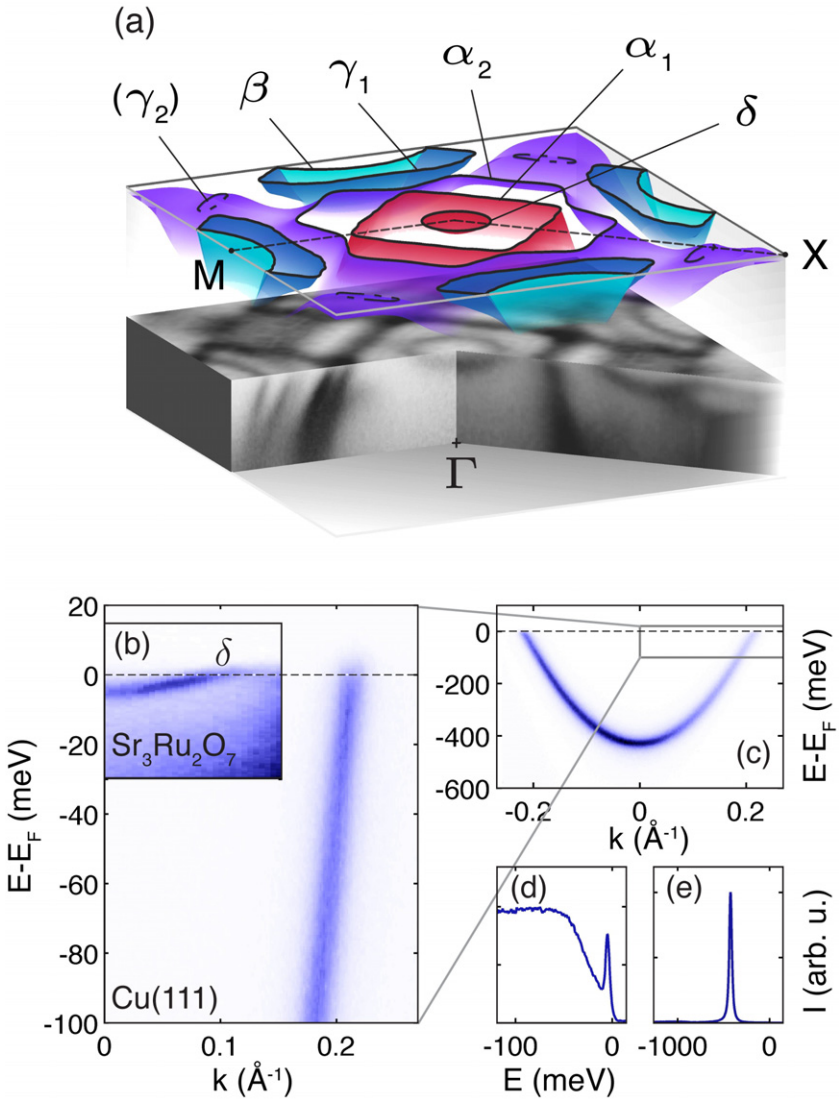

Figure 1. Renormalization of the band structure of $Sr_3Ru_2O_7$. (a) Three-dimensional photoemission intensity $I(\mathbf{k}, \omega)$ with a model of the low-energy quasiparticle band structure of $Sr_3Ru_2O_7$ obtained from a smoothing interpolation of experimentally determined initial state energies. (b), (c) False color plots (dark colors correspond to high photocurrents throughout this paper) from the L-gap surface state on Cu(111) and the δ-pocket on $Sr_3Ru_2O_7$, illustrating the marked effect of correlations on the quasiparticle dispersion in $Sr_3Ru_2O_7$. (d), (e) Spectra at the Γ point of $Sr_3Ru_2O_7$ and Cu(111), respectively.

strongly sheet *and* momentum-dependent renormalization of the Fermi velocity, reaching values more typically encountered in f-electron Kondo systems.

For the experiments presented in this paper, we used crystals grown by the floating-zone method as described in [26] with residual resistivities as low as 0.4 $\mu\Omega$ cm. Our photoemission experiments were performed using 16–57 eV photons from SSRL's beamline V-4, BESSY-II's 1^3 beamline and the SIS beamline at SLS, as well as He Iα radiation from monochromatized discharge lamps. The measurements were taken at temperatures around 8 K (figures 1, 3(a), (c)

and 4) and 1.1 K (figures 3(b) and (c)) and energy and angular resolutions of 3.5–5 meV and $\approx 0.3^\circ$, respectively. Density functional calculations within the LDA were performed using the all-electron code Wien2k including spin–orbit coupling and the pseudo-potential code Quantum Espresso [27, 28].

The low-energy electronic structure of $Sr_3Ru_2O_7$ is summarized in figure 1(a) where we show an experimental Fermi surface with a model of the low-energy quasiparticle dispersion that spans the entire Brillouin zone. The model is derived from a smoothing interpolation between $\sim 10^3$ experimentally determined initial state energies and is fully consistent with the analysis of a smaller k-space range reported in our previous work [19]. While the gross band topography resembles the LDA band structure [19, 29], the experimental quasiparticle velocities are markedly lower than the calculated bare velocities. This behavior is well known for correlated Fermi liquids and can be characterized by a renormalization constant (Fermi liquid residue) $Z_{\mathrm{FL}}^{-1} \approx v_{\mathrm{LDA}}/v_{\mathrm{exp}}$, where v_{LDA} and v_{exp} are the group velocities of bare bands as calculated within LDA and the measured quasiparticle bands at the Fermi level, respectively. However, the magnitude of Z_{FL}^{-1} in $Sr_3Ru_2O_7$ is highly unusual. Whereas most metallic 3d and 4d transition metal oxides have average mass enhancements $\gamma/\gamma_{\mathrm{LDA}} \sim 2$ [25], in $Sr_3Ru_2O_7$ Z_{FL}^{-1} reaches values up to 25 for some Fermi surface sheets as shown in figure 1. It therefore exceeds the largest values found in the single-layer compound Sr_2RuO_4, which is often described as strongly correlated, by approximately a factor of 4. We illustrate the marked influence of correlations on the quasiparticle band structure of $Sr_3Ru_2O_7$ in figures 1(b)–(e), where we compare the parabolically dispersing δ-pocket with the weakly interacting electron gas found at the Cu(111) surface [30, 31]. Both of these states have similar bare band masses of $\approx 0.4 m_e$. Yet, while the quasiparticle dispersion in Cu closely follows the bare band, the width of the δ-pocket in $Sr_3Ru_2O_7$ is reduced to ≈ 5 meV, corresponding to a renormalization constant of $Z_{\mathrm{FL}}^{-1} \approx 25$. At the same time the spectral weight of the coherent quasiparticle peak is reduced and pushed to higher energy, resulting in the characteristic 'peak-dip-hump' line shape of strongly interacting systems (figure 1(d)).

The same energy scale and equally strong band renormalization, combined with marked multi-band effects, are observed over a large k-space volume spanned by the hybridized α_2–γ_2 sheet (figures 1 and 3). For these bands of mixed xz/yz, xy orbital character (see [13]), the low-energy scale is much more important, since they span a large area in k-space and thus dominate the low-energy density of states. Several authors proposed that many properties of quantum critical materials as they are seen in $Sr_3Ru_2O_7$ and some heavy fermion systems can be explained assuming a narrow peak in the density of states close to or locked to the chemical potential [3, 5, 32, 33]. In order to test this idea for $Sr_3Ru_2O_7$ we numerically computed the quasiparticle density of states $g(\varepsilon)$ from our model of the low-energy band dispersion shown in figure 1(a), and used this function to calculate the temperature dependence of the electronic specific heat given by $C_{\mathrm{el}}(T)/T = \frac{1}{T}\frac{\partial}{\partial T}\int \varepsilon g(\varepsilon) f(\varepsilon, T)\, \mathrm{d}\varepsilon$. The result, shown in figure 2(a) assuming constant density of states above the Fermi energy, correctly reproduces the magnitude and the gross shape of $C_{el}(T)/T$ including the temperature of the maximum. Intriguingly, our data even reproduce the strong enhancement of the specific heat in an applied field (figure 2(b)). In this calculation, we use a simple, rigid band shift of the Zeeman split states. With this approach we find that the specific heat at zero-temperature peaks for a Zeeman splitting of 1.8 meV corresponding to a field of 15 T for $g = 2$. Given that our model neglects any temperature and field dependence of the many-body density of states, the agreement with direct measurements of the temperature and field dependence of the specific heat [5] is excellent. This

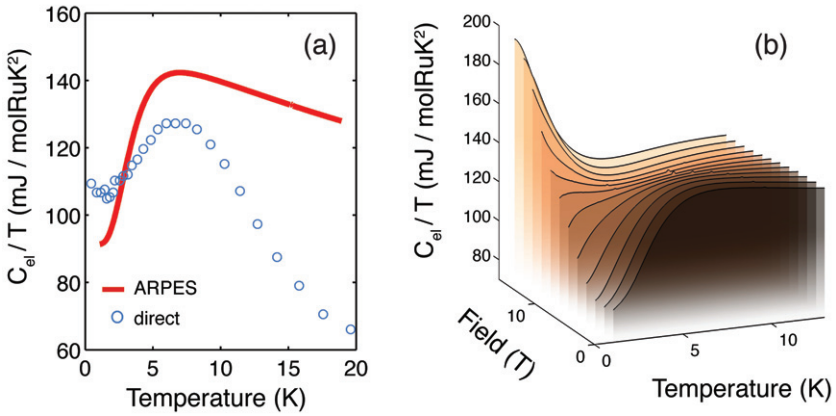

Figure 2. Calculation of the electronic specific heat from the quasiparticle band structure. (a) Comparison of the zero-field electronic specific heat from [5] with a calculation of $C_{\mathrm{el}}(T)/T = \frac{1}{T}\frac{\partial}{\partial T}\int \varepsilon g(\varepsilon) f(\varepsilon, T)\,\mathrm{d}\varepsilon$ based on our ARPES data. The density of states $g(\varepsilon)$ is computed numerically from the model of the experimental low-energy band structure shown in figure 1(a). We assumed a two-fold degeneracy of the bands around the X-point, as indicated in figure 3(c) and a constant $g(\varepsilon)$ above the Fermi level. (b) Field dependence of the specific heat from 0 to 16 T, calculated by assuming a rigid Zeeman shift of the density of states $g(\varepsilon)$.

strongly suggests that the energy scale defined by the hybridized α_2–γ_2 band, which dominates $g(\varepsilon)$, is intimately involved in quantum criticality and the formation of an electron nematic state in high field. The complex shape and orbital character of this sheet, evolving from the α_2 pocket that stems from the out-of-plane xz/yz orbital, to xy-dominated states near the X-point, highlights the need for realistic models of nematicity in $Sr_3Ru_2O_7$ to include all three t_{2g} orbitals as well as spin–orbit coupling [9, 13, 16].

For the remainder of this paper we focus on the formation of heavy d-electron quasiparticles in $Sr_3Ru_2O_7$ and their unusual Fermi surface sheet- and momentum-dependent mass enhancement. In figure 3 we show ARPES data along ΓX for selected photon energies together with the quasiparticle dispersion extracted from several measurements with different photon energies and polarizations. Attempting to describe the experimental dispersion with a minimal model, we approximate the peak positions by eight cosine bands tracking the dispersions of the fundamental bilayer split xy, xz/yz orbitals and their back-folded copies xy', xz'/yz'. (The bilayer splitting in the xy sheet is not resolved experimentally and is for illustrative purpose only.) Intriguingly, these cosine bands have very different widths with Fermi velocities varying by more than an order of magnitude. We attribute this to a combination of band structure effects and strong, orbital-dependent correlations.

The backfolding arises from a rotation of the RuO_6 octahedra around the z-axis by $\sim 7^\circ$ [34] which doubles the in-plane unit cell and folds all bands along the $(0, \pi)$–$(\pi, 0)$ line of the undistorted Brillouin zone. For the quasi-one-dimensional xz/yz orbitals, the structural distortion should merely double the number of bands and invert the dispersion of the backfolded xz'/yz' states. In contrast, backfolding of the nearly isotropic fundamental xy sheet will result in Fermi surface contours that are nearly parallel to the ΓX line and thus disperse weakly along this direction. This occurs in the LDA calculated bands as well, but the effect is far more pronounced

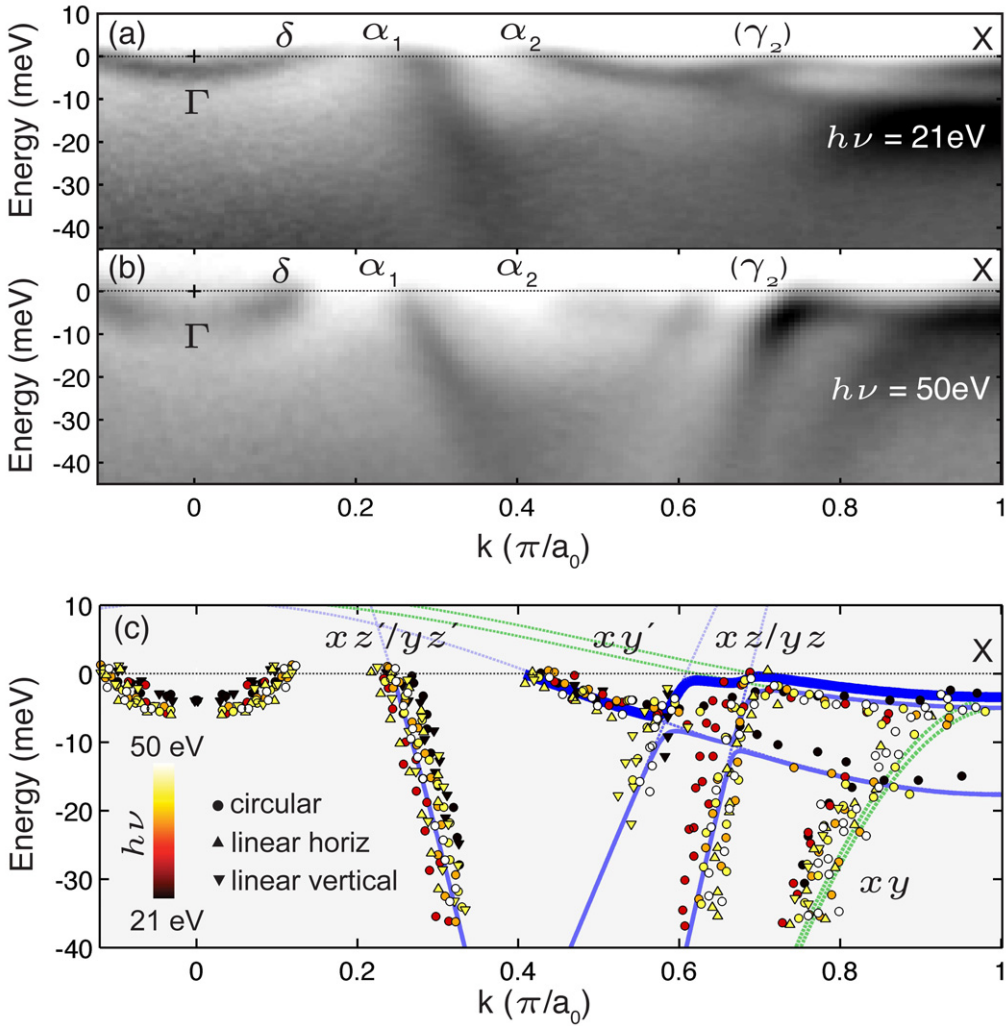

Figure 3. (a), (b) Low-energy electronic structure along ΓX. Representative cuts (see dashed line in figure 1(a)) measured with $h\nu = 21.2$ and 50 eV photons, respectively. The parallel momentum is given in units of π/a_0, where a_0 is the Ru–Ru nearest-neighbor distance. (c) Band dispersion along ΓX extracted from ARPES measurements with different photon energies and polarizations. Eight cosine dispersions track the fundamental xz/yz and xy bands and their backfolded copies (xz'/yz', xy'). The low-energy contour arising from the hybridization of these bands is indicated by a thick blue line.

in the experimental data, which we relate to many-body effects not contained in the LDA. Comparing the cosine bands of our simple model with an LDA calculation we find that the fundamental xy sheet is renormalized by a factor of ∼6, whereas the dispersion of the backfolded xy' sheet is 20–30 times smaller than in LDA, indicative of strongly enhanced correlation effects for the backfolded states which have extended flat regions and a higher density of states at very low energies. In the presence of spin–orbit coupling [35, 36] this situation naturally leads to the hybridization of very itinerant light bands and heavy states near the Fermi level, akin to the situation in f-electron heavy fermion materials. The resulting low-energy contour (figure 3(c))

remains confined to an energy range of <6 meV over an extended part of the Brillouin zone and has a complex shape with multiple saddle-point and band-edge singularities in the vicinity of the X point. This includes a band maximum at ≈ -1 meV that might lead to the putative γ_2 pocket, as discussed in our previous work [19], and, more recently, in a LDA + slave boson approach [17].

We also observe pronounced many-body effects in the out-of-plane orbitals. The xz'/yz' bands hybridize weakly to form the $\alpha_{1,2}$ Fermi surface contours as shown in figure 4(c). Within LDA these sheets have nearly isotropic bare Fermi velocities, consistent with naive expectations. However, the quasiparticle dispersion along the α_2 Fermi surface, which was also detected in spectroscopic imaging STM [21], is clearly anisotropic. This is evident from the dispersion plots shown in figures 4(a) and (b), where we overlay an LDA dispersion, globally compressed by a factor of 6, onto the data. This reproduces the Fermi velocity along ΓM but overestimates it by a factor of ≈ 3 along ΓX. The renormalization Z_{FL}^{-1} along the entire $\alpha_{1,2}$ Fermi surface sheets is visualized in panel (c) by red arrows with lengths proportional to $v_{\mathrm{LDA}}/v_{\mathrm{exp}}$, with v_{exp} extracted from a large number of cuts normal to the Fermi surface. A marked variation of Z_{FL}^{-1} corresponding to a strongly momentum-dependent self-energy along the α_2 Fermi surface is evident from the data. Such a pronounced anisotropy is unexpected for a Fermi liquid where local electron–electron correlations dominate the mass enhancement. In fact, in the absence of multi-band effects, purely local interactions lead to a self-energy that lacks any momentum dependence. Anisotropic renormalizations Z_{FL}^{-1}, as they have been reported in cuprates or cobaltates, are thus commonly attributed to coupling to bosonic modes [37–39]. And indeed, neutron scattering detected strong antiferromagnetic spin fluctuations in $Sr_3Ru_2O_7$ at energies <5 meV and wave vectors $|\mathbf{q}_1| = 0.18\pi/a_{\mathrm{t}}$ and $|\mathbf{q}_2| = 0.5\pi/a_{\mathrm{t}}$ [40, 41] that are a near perfect match to the nesting vectors connecting parallel sections of $\alpha_{1,2}$. However, our data show that the correlation between nesting and renormalization is incomplete: while $v_{\mathrm{LDA}}/v_{\mathrm{exp}}$ is clearly enhanced for the parallel sections of α_2, this is not the case for the nearly square α_1 sheet, which is as highly nested as α_2 and whose nesting vector matches the strongest antiferromagnetic fluctuations at $\mathbf{q}_2$ seen in neutron scattering. Thus, while nesting might play an important role in the physics of $Sr_3Ru_2O_7$, it cannot be the sole mechanism behind the renormalization we observe here.

On the other hand, we find a clear correlation between Z_{FL}^{-1} and the character of the wave functions at the Fermi surface. To illustrate this we introduce a simple tight-binding model describing the xz/yz orbitals of an isolated bilayer using the in-plane hopping elements (t_x, t_y) and the out-of-plane nearest (t_z) and next-nearest-neighbor (t_z') elements. The dispersion of this model along ΓX is $\varepsilon_{\mathbf{k}\pm} = 2(t_x \mp t_z')\cos k_x \pm t_z$ and its Fermi surface consists of the two sets of slightly curved light blue and pink lines in figure 4(c) which correspond to the symmetric ($|+\rangle$) and antisymmetric ($|-\rangle$) combinations of the xz/yz orbitals in the upper and lower RuO_2 plane; $|\pm\rangle = |\mathrm{upper}\rangle \pm |\mathrm{lower}\rangle$. It is evident from this analysis that the strongly and weakly renormalized bands exactly follow the $|+\rangle$ and $|-\rangle$ states, rather than the nested parallel sections of the $\alpha_{1,2}$ Fermi surfaces. We use an LDA calculation of the valence charge distribution (figures 4(d) and (e)) to elucidate the particular differences in the wave functions of the $|+\rangle$, $|-\rangle$ states in real space. The antisymmetric combination, which has a node at the apical O site in the naive tight-binding picture, indeed has little weight at this site but hybridizes with in-plane O p_z states, whereas the symmetric combination hybridizes strongly with apical O $p_{x,y}$ states but has little weight on the in-plane O. This has a moderate influence on the bare band width along ΓX which is around 1.6 eV for the antisymmetric and 0.9 eV for the symmetric combination.

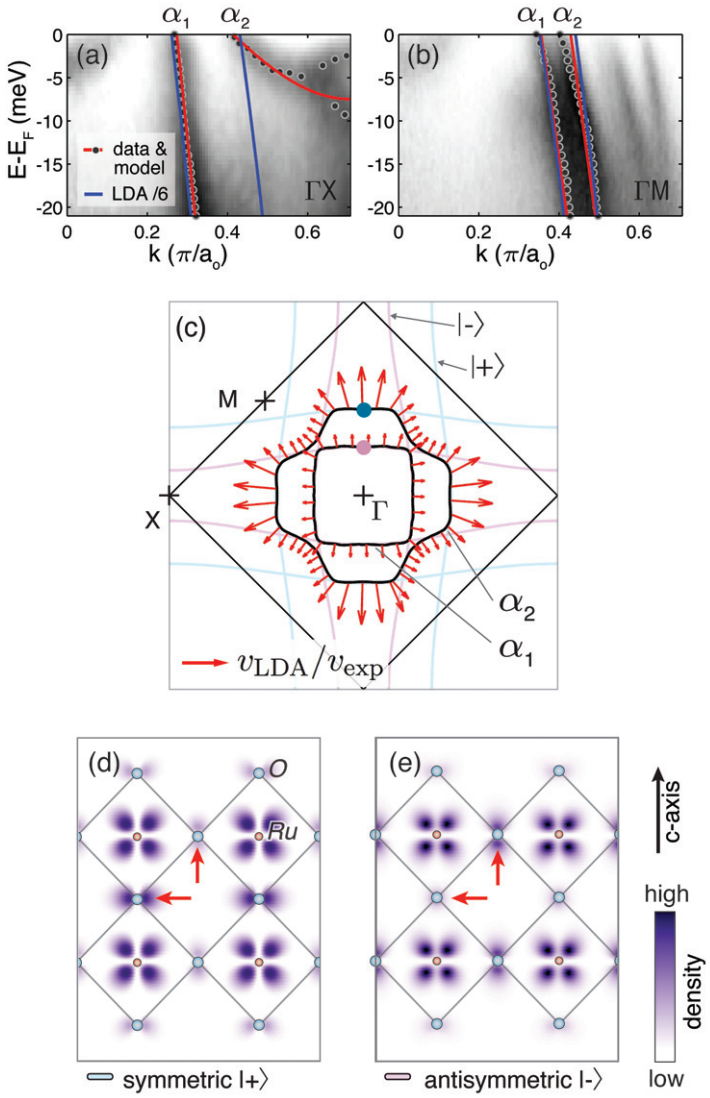

Figure 4. Anisotropic renormalization of the $\alpha_{1,2}$ Fermi surface sheet. (a), (b) ARPES data along ΓX and ΓM with a globally compressed LDA calculation (blue) and a tight-binding model (red) overlaid. Small shifts in k ($\sim 0.05\pi/a_0$) were applied to the LDA bands in order to match the experimental Fermi crossings, and the hybridization of the LDA bands has been removed. (c) Experimentally determined renormalization along the $\alpha_{1,2}$ Fermi surfaces. Red arrows are proportional to $Z_{\mathrm{FL}}^{-1} = v_{\mathrm{LDA}}/v_{\mathrm{exp}}$, i.e. longer arrows indicate a higher renormalization constant. The bilayer-split fundamental bands from the one-dimensional d_{xz}, d_{yz} orbitals before hybridization are indicated in blue (symmetric $|+\rangle$) and pink (antisymmetric $|-\rangle$). (d), (e) Valence charge density distribution for the highly and weakly renormalized states at k-points on the symmetric and antisymmetric Fermi surfaces (dots in (c)). The arrows highlight the different degree of hybridization with in-plane O p_z and apical O p_x orbitals.

Our photoemission results suggest that correlations markedly amplify this difference, possibly by reducing the effective in-plane hopping for the $|+\rangle$ states of the many-body system with little weight on in-plane oxygen. Within our empirical tight-binding picture, the relative width $r = W^-/W^+$ of the $|-\rangle$ and $|+\rangle$ bands is controlled by the ratio $t_z'/t_x = (r-1)/(r+1)$ between the diagonal inter-layer hopping and the dominant in-plane hopping. The LDA dispersion can be described with $t_z'/t_x \approx 0.28$, similar to what is used for many theoretical models[13]. However, the fit shown in figures 4(a) and (b) as a red line suggests that t_z'/t_x is as high as 0.85 in the many-body dispersion, which should have a profound effect on the behavior of the large α_2 Fermi surface sheet in external fields. We point out that strong variations of the orbital character are not restricted to α_2 but are observed for most Fermi surface sheets including γ_1 and the putative γ_2 pocket. The complexity added over Sr_2RuO_4 by the RuO_2 bilayer in $Sr_3Ru_2O_7$ goes far beyond simple band structure effects and includes substantially altered effects of many-body interactions, which might hold the clue to their remarkably different thermodynamic properties.

In conclusion, we illustrated how orbital-dependent renormalization, backfolding and hybridization lead to the formation of heavy d-electron quasiparticles in $Sr_3Ru_2O_7$ with a strongly structured low-energy density of states. We further argued that, in multi-band systems with strong orbital mixing along the Fermi surface such as $Sr_3Ru_2O_7$, local electron correlations can cause a pronounced anisotropy in the mass enhancement, which should be included in future more realistic models of the electron nematic phase. We expect that both of these effects are of general relevance to 4d transition metal oxides and other strongly correlated multi-band systems.

Acknowledgments

We gratefully acknowledge discussions with A Georges, M S Golden, R G Hennig, C Hooley, J Mravlje, A W Rost, S C Sundar and J Zaanen. This work has been supported by the European Research Council, the Scottish Funding Council and the UK EPSRC. SSRL is operated by the DOE's office of Basic Energy Science. Work by MHF, E-AK, KMS, CJF and JV was supported by the Cornell Center for Materials Research with funding from the NSF MRSEC program (DMR-1120296). Work by MPA during the write-up of this paper was supported by an ETH Fellowship.

References

[1] Grigera S A, Perry R S, Schofield A J, Chiao M, Julian S R, Lonzarich G G, Ikeda S I, Maeno Y, Millis A J and Mackenzie A P 2001 *Science* **294** 329–32

[2] Borzi R A, Grigera S A, Farrell J, Perry R S, Lister S J S, Lee S L, Tennant D A, Maeno Y and Mackenzie A P 2007 *Science* **315** 214

[3] Farrell J, Perry R S, Rost A, Mercure J F, Kikugawa N, Grigera S A and Mackenzie A P 2008 *Phys. Rev.* B **78** 180409

[4] Rost A W, Perry R S, Mercure J-F, Mackenzie A P and Grigera S A 2009 *Science* **3251** 1360

[5] Rost A W, Grigera S A, Bruin J A N, Perry R S, Tian D, Raghu S, Kivelson S A and Mackenzie A P 2011 *Proc. Natl Acad. Sci. USA* **108** 16549

[6] Binz B and Sigrist M 2004 *Europhys. Lett.* **65** 816

[13] The nearly identical LDA Fermi velocity of the $\alpha_{1,2}$ sheets along ΓX results from a compensation of the k-dependence of the group velocity along the band and the different band widths of the $|+\rangle$, $|-\rangle$ states and is thus accidental.

[7] Kee H-Y and Kim Y B 2005 *Phys. Rev.* B **71** 184402
[8] Yamase H and Katanin A A 2007 *J. Phys. Soc. Japan* **76** 073706
[9] Raghu S, Paramekanti A, Kim E-A, Borzi R A, Grigera S A, Mackenzie A P and Kivelson S A 2009 *Phys. Rev.* B **79** 214402
[10] Berridge A M, Green A G, Grigera S A and Simons B D 2009 *Phys. Rev. Lett.* **102** 136404
[11] Lee W-C and Wu C 2009 *Phys. Rev. Lett.* **103** 176101
[12] Fischer M H and Sigrist M 2010 *Phys. Rev.* B **81** 064435
[13] Puetter C M, Rau J G and Kee H-Y 2010 *Phys. Rev.* B **81** 081105(R)
[14] Fradkin E, Kivelson S A, Lawler M J, Eisenstein J P and Mackenzie A P 2010 *Annu. Rev. Condens. Matter Phys.* **1** 53
[15] Behrmann M, Piefke C and Lechermann F 2012 *Phys. Rev.* B **86** 045130
[16] Puetter C M, Swiecicki S D and Kee H-Y 2012 *New J. Phys.* **14** 053027
[17] Piefke C and Lechermann F 2011 *Phys. Status Solidi* b **248** 2269
[18] Ikeda S-I, Maeno Y, Nakatsuji S, Kosaka M and Uwatoko Y 2000 *Phys. Rev.* B **62** R6089
[19] Tamai A *et al* 2008 *Phys. Rev. Lett.* **101** 026407
[20] Iwaya K *et al* 2007 *Phys. Rev. Lett.* **99** 057208
[21] Lee J, Allan M P, Wang M A, Farrell J, Grigera S A, Baumberger F, Davis J C and Mackenzie A P 2009 *Nature Phys.* **5** 800
[22] Borzi R A, Grigera S A, Perry R S, Kikugawa N, Kitagawa K, Maeno Y and Mackenzie A 2004 *Phys. Rev. Lett.* **92** 216403
[23] de' Medici L, Mravlje J and Georges A 2011 *Phys. Rev. Lett.* **107** 256401
[24] Mravlje J, Aichhorn M, Miyake T, Haule K, Kotliar G and Georges A 2011 *Phys. Rev. Lett.* **106** 096401
[25] Georges A, de'Medici L and Mravlje J 2013 *Annu. Rev. Condens. Matter Phys.* **4** 137–78
[26] Perry R S and Maeno Y 2004 *J. Cryst. Growth* **271** 134
[27] Blaha P, Schwarz K, Madsen G K H, Kvasnicka D and Luitz J 2001 *WIEN2K An Augmented Plane Wave + Local Orbitals Program for Calculating Crystal Properties* (Vienna: Techn. Universität Wien) (available at www.wien2k.at/index.html)
[28] Giannozzi P *et al* 2009 *J. Phys.: Condens. Matter* **21** 395502
[29] Singh D J and Mazin I I 2001 *Phys. Rev.* B **63** 165101
[30] Gartland P O and Slagsvold B J 1975 *Phys. Rev.* B **12** 4047
[31] F Reinert, G Nicolay, S Schmidt, D Ehm and S Hüfner 2001 *Phys. Rev.* B **63** 115415
[32] Daou R, Bergemann C and Julian S R 2006 *Phys. Rev. Lett.* **96** 026401
[33] Pfau H, Daou R, Brando M and Steglich F 2012 *Phys. Rev.* B **85** 035127
[34] Shaked H, Jorgensen J D, Chmaissem O, Ikeda S and Maeno Y 2000 *J. Solid State Chem.* **154** 361–7
[35] Liu G-Q, Antonov V N, Jepsen O and Andersen O K 2008 *Phys. Rev. Lett.* **101** 026408
[36] Haverkort M W, Elfimov I S, Tjeng L H, Sawatzky G A and Damascelli A 2008 *Phys. Rev. Lett.* **101** 026406
[37] Gromko A D, Fedorov A V, Chuang Y D, Koralek J D, Aiura Y, Yamaguchi Y, Oka K, Ando Y and Dessau D S 2003 *Phys. Rev.* B **68** 174520
[38] Cuk T *et al* 2004 *Phys. Rev. Lett.* **93** 117003
[39] Geck J *et al* 2007 *Phys. Rev. Lett.* **99** 046403
[40] Capogna L, Forgan E M, Hayden S M, Wildes A, Duffy J A, Mackenzie A P, Perry R S, Ikeda S, Maeno Y and Brown S P 2003 *Phys. Rev.* B **67** 012504
[41] Ramos S *et al* 2008 *Physica* B **403** 1270